Insights into the formation of OB associations: an examination of key parameters

S. Ortega[1], M. Bascuñán[1], S. Villanova[1] & P. Assmann[1]

[1] *Universidad de Concepción, Chile*

Resumen / Las asociaciones OB son conglomerados estelares no ligados que albergan todo tipo de estrellas, destacándose las de tipo OB. Este grupo estelar resulta de particular interés debido a su idoneidad como entornos para el estudio del proceso de formación estelar. En este trabajo, evolucionamos cúmulos estelares jóvenes con el propósito de determinar los parámetros fundamentales que propiciarían la formación de una asociación OB. Para generar las condiciones iniciales, empleamos el código MCLUSTER para introducir fractalidad en la distribución estelar. Además, ajustamos un radio de media masa de 1 pc, una función inicial de masa de Kroupa y un 10 % de estrellas binarias. Posteriormente, utilizamos el código NBODY6++GPU para evolucionar el cúmulo, incorporando un potencial de fondo que representara el gas residual de la formación estelar. El gas se modeló como una esfera de Plummer que, después de un tiempo característico, comenzó a reducir su masa, simulando así la expulsión de gas de los cúmulos estelares jóvenes. Se exploraron dos escenarios: uno con una expulsión instantánea y otro con una expulsión lenta de la masa de gas. Nuestros hallazgos revelan que, tras 10 millones de años, las simulaciones con expulsión instantánea de gas lograron un radio promedio para el cúmulo de 28.8 pc. Este resultado se sitúa en concordancia con el tamaño característico de una asociación OB, validando así nuestros modelos como posible escenario de evolución de estos sistemas estelares.

Abstract / OB associations are unbound stellar clusters that house a variety of stars, with a particular emphasis on those classified as OB types. This stellar group is of specific interest due to its suitability as an environment for studying the star formation process. In this study, we evolved young star clusters with the aim of determining the fundamental parameters that would lead to the formation of an OB association. We employed the MCLUSTER code to introduce fractality into the stellar distribution to generate initial conditions. Additionally, we adjusted a half-mass radius of 1 pc, an initial mass function following Kroupa, and included 10% binary stars. Subsequently, we used the NBODY6++GPU code to evolve the cluster, incorporating a background potential representing residual gas from star formation. The gas was modeled as a Plummer sphere, which, after a characteristic time, began to reduce its mass, simulating the expulsion of gas from young star clusters. Two scenarios were explored: one with instantaneous gas expulsion and another with a slow expulsion of gas mass. Our findings reveal that, after 10 million years, simulations with instantaneous gas expulsion achieved an average cluster radius of 28.8 pc. This result aligns with the characteristic size of an OB association, thereby validating our models as a possible scenario for the evolution of these stellar systems.

Keywords / Galaxy: kinematics and dynamics — open clusters and associations: general — stars: evolution — methods: numerical

1. Introduction

OB associations, situated within the Milky Way, constitute a diverse collection of stars, with the OB types taking center stage, signifying the youthful nature of these stellar clusters. This inherent youthfulness makes OB associations valuable arenas for investigating recent star formation and the distribution patterns of young stars (Wright, 2020).

The formation mechanisms of OB associations remain a subject of discussion, with two primary models seeking to explain their origins. The monolithic model suggests that OB associations evolve from young clusters, expanding due to the expulsion of residual gas resulting from stellar birth processes, driven by phenomena such as stellar winds, UV radiation, and supernova explosions. Alternatively, the hierarchical model proposes that stars can form in regions of overdensity without adhering to a specific pattern, and their current distribution reflects the conditions of their birth (Carraro, 2020).

Typically, OB associations exhibit sizes ranging from $10 - 500$ pc (Melnik & Dambis, 2017) and maintain low densities (< 0.1 $M_\odot$ pc^{-3}) (Wright, 2020). Melnik & Dambis (2020) calculated a median stellar mass of 8.1×10^3 $M_\odot$ and an average of 22 stars with a mass greater than 20 $M_\odot$ based on their study of 28 OB associations. However, each association showcases unique features; for instance, Beccari et al. (2018) identified two stellar populations in the Vela OB2 association, aged 10 Myr and 30 Myr, respectively. Similarly, Cantat-Gaudin et al. (2019) identified 11 star subgroups in Vela OB2 based on proper motions and parallaxes. Additionally, certain OB associations like

Research article

Table 1. Initial stellar parameters set in McLuster.

Parameter	Option
Stars number	10 000
Density profile	Homogeneous sphere
Half mass radius	1 pc
Fractal dimension	1.6
Initial mass function	Kroupa
Binary fraction	0.1

Per OB1, Car OB1, Sgr OB1, Gem OB1, Ori OB1, and Sco OB1 exhibit signs of expansion, as analyzed using Gaia DR2 proper motions by Melnik & Dambis (2020).

In this study, we employ the McLuster (Küpper et al., 2011) * code along with N-body simulations by using Nbody6++GPU (Wang et al., 2015) ** code to discern the fundamental parameters influencing the formation of OB associations. Adopting a monolithic scenario in our model, we evolve stellar clusters over time, considering the individual stellar evolution of each star, and incorporate a background gas potential to simulate the effects of the expulsion of the cluster's initial gas.

2. Simulations

2.1. Generation of initial conditions

For this study we utilize the McLuster code, which enables us to derive clusters from their nascent stages of formation. The McLuster code serves as a tool for generating the initial conditions of clusters by adjusting parameters related to spatial and mass distribution.

2.1.1. Setup

Our initial stellar distribution comprises a young cluster with 10 000 stars, with 10% of them existing as primordial binary stars. These stars are spatially distributed within a homogeneous sphere exhibiting maximum fractality, a design chosen to generate clusters without adhering to predefined patterns. Additionally, we set a half-mass radius of 1 pc and adopt a Kroupa initial mass function (IMF) within a mass range spanning from 0.08 to 40 $M_\odot$. This results in a total stellar mass (M_{st}) of 5 056 $M_\odot$ and a cluster radius of 1.6 pc.
The parameters mentioned above are summarized in Table 1. In Fig. 1, we can see the cluster, generated with the McLuster code, that will be evolved in Nbody6++GPU to analyze its evolution, which could lead to the formation of OB association.

2.2. N-body simulations

We utilize Nbody6++GPU to steer the dynamical evolution of these young clusters. During the simulations,

*https://github.com/ahwkuepper/mcluster
**https://github.com/nbodyx/Nbody6ppGPU
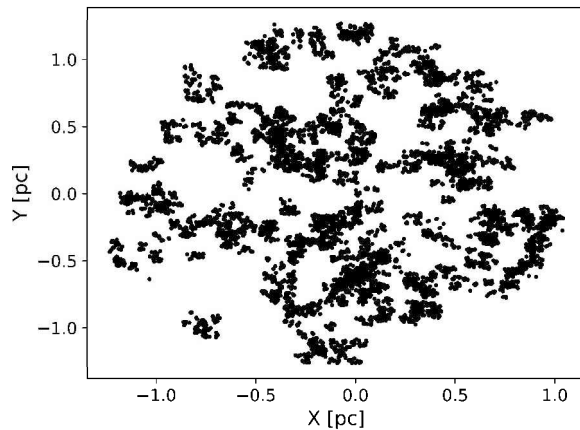
Fig. 1. Initial two dimensional distribution of the star cluster with substructure from a homogeneous sphere.

we consider the stellar evolution of each star complemented by the incorporation of a background gas potential into the model.

2.2.1. Background potential

In our simulations, we incorporate a background potential arising from residual gas generated during star formation. This potential is precisely modeled by adjusting parameters in accordance with Nbody6++GPU keywords: total mass of the Plummer gas sphere (MP), Plummer scale factor (AP), decay time for gas expulsion ($MPDOT$), and initiation time for gas expulsion ($TDELAY$).

To calculate the total gas mass ($M = MP$), we employ Eq. 1, which represents the mass contained within a radius r. Here, "a" denotes the Plummer radius, and "r" is the cluster's radius:

$$M(r) = M \left(1 + \frac{a^2}{r^2}\right)^{-3/2}. \tag{1}$$

The gas distribution within the cluster ($M(r) = M_g$) aligns with the adjusted star formation efficiency (SFE) (Farias et al., 2015), ensuring consistency throughout the distribution:

$$SFE = \frac{M_{st}}{M_{st} + M_g}. \tag{2}$$

The evolution of gas mass in the code adheres to Eq. 3, where $MP0$ signifies the initial mass of the Plummer gas sphere (MP). This equation is exclusively applicable during the gas expulsion phase:

$$MP(T) = \frac{MP0}{(1 + MPDOT(T - TDELAY))}. \tag{3}$$

2.3. Evolution of the simulations

All simulations within this investigation adhere strictly to the initial parameters outlined in Table 1. The SFE of 10% yields a total mass for the Plummer gas sphere

equivalent to $75\,843$ M$_\odot$, with the Plummer scale factor (AP) precisely set at 1 pc.

To evaluate the impact for gas expulsion on the evolution of the cluster, we systematically investigate two extreme scenarios for the decay time of the gas. In the initial scenario, where $MPDOT$ is set to $10\,000$ (expressed in N-body units), nearly 99% of the total gas mass is expelled within an exceptionally brief timeframe of 1.8×10^{-3} Myr after $TDELAY$. Conversely, in the second scenario with $MPDOT$ adjusted to 0.1, a substantial 50% reduction in gas mass is observed 1.8 Myr after $TDELAY$. In both instances, the initiation of gas expulsion occurs precisely at 4.5 Myr.

Finally, we performed five simulations per set, and the adjusted parameters for background gas are summarized in Table 2.

3. Results

The ensuing section delineates the outcomes derived from the performed numerical simulations. The results are obtained from the average of each simulation set.

Figure 2 shows the evolution of the Lagrangian radius. In the top panel, the average from five simulations of Sim 1 reveals an immediate expansion of cluster shells following gas expulsion. Conversely, the bottom panel displays the average from five simulations of Sim 2, depicting a slower expansion resulting in a more concentrated cluster.

Using the Lagrangian radius, we define the core radius as the boundary containing 20% of the cluster's mass and the cluster radius as the boundary containing 80% of the cluster's mass. The simulation outcomes, including core and cluster radii, are detailed in Table 3.

Our focused analysis centers on the simulations at 10 Myr and 20 Myr, representing the typical ages of OB associations according to Wright (2020). Parameters under examination include the core radius (R_{core}), the count of OB stars within the core radius ($N_{OB,core}$), and the count of stars exceeding 20 M$_\odot$ within the core radius ($N_{20,core}$). Additionally, we evaluate the cluster radius ($R_{cluster}$), the count of OB stars within the cluster radius ($N_{OB,cluster}$), and the count of stars with a mass greater than 20 M$_\odot$ within the cluster radius ($N_{20,cluster}$).

4. Conclusions

At 10 Myr, simulations in Sim 1 resulted in an average cluster radius of 28.8 pc, falling within the observed size range of OB associations ($10 - 500$ pc). This outcome suggests that adjusting a higher $MPDOT$ than that in Sim 2 is necessary when comparing our simulations with OB associations of this age. However, by 20 Myr, both simulation sets reached sizes representative of OB associations.

Additionally, both sets of simulations yielded comparable stars with masses exceeding 20 M$_\odot$, both within the core and the entire cluster. It is noteworthy, however, that in all cases, this count of stars remains considerably lower than Melnik & Dambis (2020) reported, and even
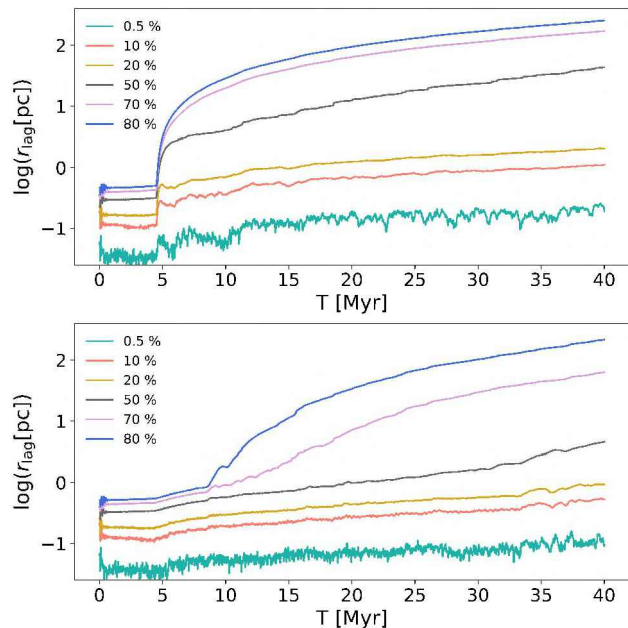
Fig. 2. Evolution of the Lagrangian radius. Each color curve indicates radius values that contain a certain percentage of the total mass of the cluster. The *upper panel* corresponds to Sim 1 and the *lower panel* represents Sim 2.

at 20 M$_\odot$ our model does not yield any such stars. This discrepancy is attributed to our focus on the monolithic model, having a group of pre-existing stars, making it improbable to find extremely massive stars after 10 Myr due to stellar evolution.

Notably, the most massive stars in the cluster are the most likely to be observed in reality, due to their magnitude values. For this reason, the analysis of the number of OB stars and stars with masses greater than 20 M$_\odot$ presented in Table 3 was performed to approximate their distribution throughout the cluster.

In conclusion, we identify the decay time for gas expulsion ($MPDOT$) as a pivotal parameter in our model to emulate the characteristics of OB associations, such as their sizes. Future endeavors will explore the variation of parameters, including the initial mass of the cluster and the half-mass radius, to refine our model and gain deeper insights into the essential factors influencing the formation of OB associations.

References

Beccari G., et al., 2018, MNRAS, 481, L11
Cantat-Gaudin T., et al., 2019, A&A, 621, A115
Carraro G., 2020, Boletin de la Asociacion Argentina de Astronomia La Plata Argentina, 61C, 11
Farias J.P., et al., 2015, MNRAS, 450, 2451
Küpper A.H.W., et al., 2011, MNRAS, 417, 2300
Melnik A.M., Dambis A.K., 2017, MNRAS, 472, 3887
Melnik A.M., Dambis A.K., 2020, MNRAS, 493, 2339
Wang L., et al., 2015, MNRAS, 450, 4070

Table 2. Summary of simulation sets, including gas potential.

Simulation	SFE [%]	M_g [M$_\odot$]	r [pc]	AP [pc]	MP [M$_\odot$]	$MPDOT$	$TDELAY$ [Myr]
Sim 1	10	45 506.79	1.6	1	75 842.62	10 000	4.5
Sim 2	10	45 506.79	1.6	1	75 842.62	0.1	4.5

Table 3. Simulation results.

Simulation	T [Myr]	R_{core} [pc]	$N_{OB,core}$	$N_{20,core}$	$R_{cluster}$ [pc]	$N_{OB,cluster}$	$N_{20,cluster}$
Sim 1	10	0.7	102	3	28.8	256	3
	20	1.3	106	0	94.3	281	0
Sim 2	10	0.3	96	2	1.6	295	3
	20	0.4	113	0	30.5	288	0

Wright N.J., 2020, NewAR, 90, 101549